Electronic Supplementary Information (ESI) for

Facile access to *N*-substituted anilines via dehydrogenative aromatization catalysis over supported gold–palladium bimetallic nanoparticles

Kento Taniguchi, Xiongjie Jin, Kazuya Yamaguchi and Noritaka Mizuno*

Department of Applied Chemistry, School of Engineering, The University of Tokyo, 7-3-1 Hongo, Bunkyo-ku, Tokyo 113-8656, Japan.
Email: tmizuno@mail.ecc.u-tokyo.ac.jp

Effect of catalyst preparation methods

As described in Experimental section, Au–Pd/Al_2O_3 used in this study was prepared by "co-precipitation" of gold and palladium hydroxide precursors on Al_2O_3, followed by the reduction using H_2. By this procedure, Au–Pd alloy nanoparticles with the average size of 2.9 nm were formed on the support (Fig. 1). This Au–Pd/Al_2O_3 catalyst showed the high catalytic performance for the present dehydrogenative aromatization. Under the conditions described in Table 1, the desired aniline **3aa** was produced in 59% yield (Table 1, entry 3).

One referee pointed out the importance of the preparation method for such kinds of bimetallic catalysts. Thus, according to the comment, we prepared two Au–Pd/Al_2O_3 catalysts with different orders of the component supporting (see the following **Methods A** and **B**), and their catalytic performances were examined for the dehydrogenative aromatization of **1a** with **2a** under the conditions described in Table 1.

(Method A) Initially, Pd/Al_2O_3 was prepared. Then, the gold hydroxide species was precipitated onto Pd/Al_2O_3, followed by the H_2 reduction (Au: 0.109 mmol g^{-1}, Pd: 0.120 mmol g^{-1}). The notation of this catalyst is Au–Pd/$Al_2O_{3(Pd\rightarrow Au)}$. It was confirmed by the TEM analysis that the average size of nanoparticles in Au–Pd/$Al_2O_{3(Pd\rightarrow Au)}$ was 3.5 nm (Fig. S6). When using Au–Pd/$Al_2O_{3(Pd\rightarrow Au)}$ for the dehydrogenative aromatization of **1a** with **2a**, 62% yield of **3aa** was obtained. Thus, the catalytic performance of Au–Pd/$Al_2O_{3(Pd\rightarrow Au)}$ was almost the same as that of Au–Pd/Al_2O_3 (59% yield, Table 1, entry 3).

(Method B) Initially, Au/Al_2O_3 was prepared. Then, the palladium hydroxide species was precipitated onto Au/Al_2O_3, followed by the H_2 reduction (Au: 0.115 mmol g^{-1}, Pd: 0.128 mmol g^{-1}). The notation of this catalyst is Au–Pd/$Al_2O_{3(Au\rightarrow Pd)}$. As shown in Fig. S7a, the average size of nanoparticles (6.3 nm) and the size distribution were relatively larger than those of Au–Pd/Al_2O_3 and Au–Pd/$Al_2O_{3(Pd\rightarrow Au)}$. It was revealed by the HAADF-STEM and EDS analyses that the larger particles (>5 nm) were mainly core–shell (Au_{core}–Pd_{shell}) and palladium nanoparticles and that the smaller ones (<3 nm) were predominantly palladium (Fig. S7b−d). Therefore, **Method B** is not suitable for preparation of Au–Pd

alloy nanoparticles. When the reaction was performed using Au–Pd/$Al_2O_{3(Au\rightarrow Pd)}$, the desired **3aa** was obtained in 39% yield, and the performance was significantly inferior to those of Au–Pd/Al_2O_3 and Au–Pd/$Al_2O_{3(Pd\rightarrow Au)}$.

Compound data

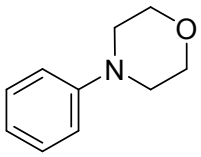

3aa (CAS registry number: 92-53-5)

4-Phenylmorpholine (3aa). ^{1}H NMR (500 MHz, $CDCl_3$, 25 °C, TMS): δ = 7.28–7.25 (m, 2H), 6.91–6.86 (m, 3H), 3.84 (t, J = 4.5 Hz, 4H), 3.13 (t, J = 4.3 Hz, 4H); ^{13}C {^{1}H} NMR (125 MHz, $CDCl_3$, 25 °C, TMS): δ = 151.5, 129.4, 120.3, 116.0, 67.2, 49.6; MS (70 eV, EI): *m/z* (%): 163 (58) [M^+], 164 (6), 162 (5), 132 (6), 106 (10), 105 (100), 104 (41), 91 (5), 78 (5), 77 (30), 51 (11).

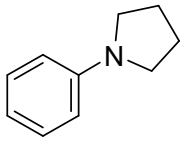

3ab (CAS registry number: 4096-21-3)

1-Phenylpyrrolidine (3ab). MS (70 eV, EI): *m/z* (%): 147 (76) [M^+], 148 (8), 146 (100), 144 (6), 119 (8), 118 (5), 104 (18), 91 (49), 77 (29), 51 (10), .

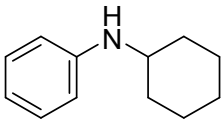

3ac (CAS registry number: 1821-36-9)

***N*-Cyclohexylbenzenamine (3ac).** ^{1}H NMR (500 MHz, $CDCl_3$, 25 °C, TMS): δ = 7.16–7.12 (m, 2H), 6.64 (tt, J = 7.5 and 1.0 Hz, 1H), 6.58–6.56 (m, 2H), 3.49 (brs, 1H), 3.26–3.21 (m, 1H), 2.06–2.03 (m, 2H), 1.77–1.72 (m, 2H), 1.67–1.61 (m, 1H), 1.40–1.31 (m, 2H), 1.25–1.09 (m, 3H); ^{13}C {^{1}H} NMR (125 MHz, $CDCl_3$, 25 °C, TMS): δ = 147.7, 129.5, 117.1, 113.4, 51.9, 33.8, 26.2, 25.3; MS (70 eV, EI): *m/z* (%): 175 (34) [M^+], 133 (12), 132 (100), 119 (12), 118 (15), 117 (9), 106 (9), 93 (12), 91 (5), 77 (10).

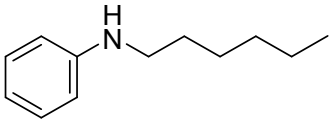

3ad (CAS registry number: 4746-32-1)

***N*-Hexylbenzenamine (3ac).** MS (70 eV, EI): *m/z* (%): 177 (15) [M^+], 107 (8), 106 (100), 79 (5), 77 (9).

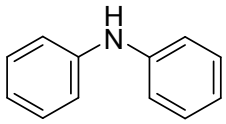

3ae (CAS registry number: 122-39-4)

***N*-Phenylbenzenamine (3ae).** ^{1}H NMR (500 MHz, $CDCl_3$, 25 °C, TMS): δ = 7.27–7.24 (m, 4H), 7.06 (d, J = 8.5 Hz, 4H), 6.92 (t, J = 7.0 Hz, 2H), 5.67 (brs, 1H); ^{13}C {^{1}H} NMR (125 MHz, $CDCl_3$, 25 °C, TMS): δ = 143.4, 130.0, 121.3, 118.1; MS (70 eV, EI): *m/z* (%): 169 (100) [M^+], 170 (13), 168 (58), 167 (30), 166 (5), 141 (5), 115 (5), 84 (16), 77 (11), 66 (8), 65 (7), 51 (12).

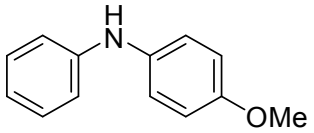

3af (CAS registry number: 1208-86-2)

4-Methoxy-*N*-phenylbenzenamine (3af). MS (70 eV, EI): *m/z* (%): 199 (75) [M^+], 200 (11), 185 (13), 184 (100), 167 (5), 155 (5), 154 (9), 129 (15), 128 (12), 77 (12), 51 (7).

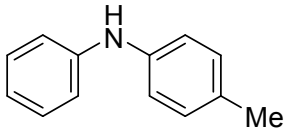

3ag (CAS registry number: 620-84-8)

4-Methyl-*N*-phenylbenzenamine (3ag). MS (70 eV, EI): *m/z* (%): 183 (100) [M^+], 184 (15), 182 (53), 180 (7), 168 (6), 167 (19), 91 (16), 90 (6), 77 (10), 65 (5), 51 (5).

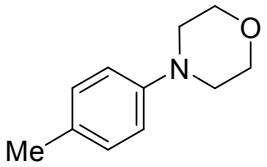

3ba (CAS registry number: 3077-16-5)

4-(4-Methylphenyl)morpholine (3ba). MS (70 eV, EI): *m/z* (%): 177 (49) [M^+], 178 (6), 120 (10), 119 (100), 118 (28), 91 (44), 90 (5), 89 (5), 77 (5), 65 (15), 51 (5).

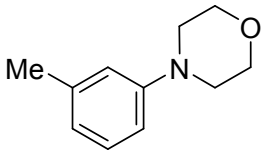

3ca (CAS registry number: 7025-91-4)

4-(3-Methylphenyl)morpholine (3ca). MS (70 eV, EI): *m/z* (%): 177 (47) [M^+], 178 (6), 146 (5), 120 (10), 119 (100), 118 (33), 92 (5), 91 (34), 89 (5), 77 (5), 65 (16).

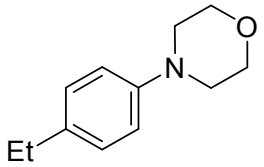

3da (CAS registry number: 1207717-24-5)

4-(4-Ethylphenyl)morpholine (3ca). MS (70 eV, EI): *m/z* (%): 191 (78) [M^+], 192 (10), 190 (6), 177 (5), 176 (39), 134 (11), 133 (100), 132 (15), 130 (6), 119 (12), 118 (98), 117 (9), 105 (19), 104 (9), 103 (10), 91 (16), 90 (8), 89 (6), 79 (8), 78 (8), 77 (19), 65 (8), 51 (7).

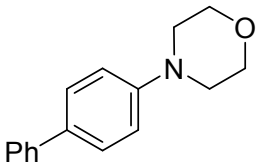

3ea (CAS registry number: 169963-54-6)

4-[1,1'-biphenyl]-4-ylmorpholine (3ea). MS (70 eV, EI): *m/z* (%): 239 (86) [M^+], 240 (15), 238 (5), 182 (15), 181 (100), 180 (22), 167 (6), 154 (5), 153 (27), 152 (37), 151 (9), 147 (5), 90 (21), 77 (8), 76 (15), 73 (18).

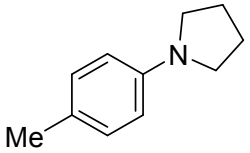

3bb (CAS registry number: 54104-82-4)

1-(4-Methylphenyl)pyrrolidine (3bb). MS (70 eV, EI): *m/z* (%): 161 (75) [M^+], 162 (8), 160 (100), 133 (5), 118 (16), 117 (6), 105 (43), 91 (23), 77 (5), 65 (11).

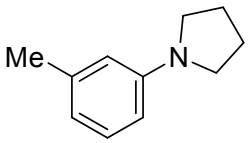

3cb (CAS registry number: 71982-22-4)

1-(3-Methylphenyl)pyrrolidine (3cb). MS (70 eV, EI): *m/z* (%): 161 (73) [M^+], 162 (8), 160 (100), 133 (6), 118 (13), 117 (5), 106 (5), 105 (43), 91 (23), 77 (5), 65 (12).

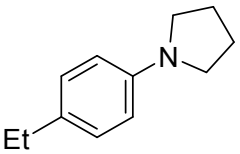

3db (CAS registry number: 872874-50-5)

1-(4-Ethylphenyl)pyrrolidine (3db). MS (70 eV, EI): *m/z* (%): 175 (52) [M^+], 176 (7), 174 (28), 161 (12), 160 (100), 132 (5), 130 (5), 119 (13), 118 (10), 117 (5), 91 (8), 77 (7).

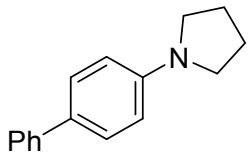

3eb (CAS registry number: 265991-28-4)

1-[1,1'-biphenyl]-4-ylpyrrolidine (3eb). MS (70 eV, EI): *m/z* (%): 223 (100) [M^+], 224 (17), 222 (81), 180 (8), 167 (25), 165 (6), 153 (14), 152 (23), 151 (6), 112 (6), 90 (6), 76 (8).

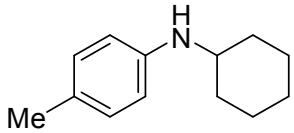

3bc (CAS registry number: 10386-93-3)

***N*-Cyclohexyl-4-methylbenzenamine (3bc).** MS (70 eV, EI): *m/z* (%): 189 (38) [M^+], 190 (5), 147 (13), 146 (100), 133 (15), 132 (10), 131 (14), 130 (7), 120 (9), 118 (7), 107 (10), 106 (14), 91 (10), 77 (6), 65 (5).

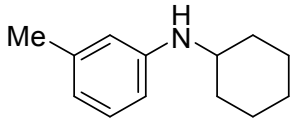

3cc (CAS registry number: 65021-67-2)

***N*-Cyclohexyl-3-methylbenzenamine (3cc).** MS (70 eV, EI): *m/z* (%): 189 (38) [M^+], 190 (6), 147 (13), 146 (100), 133 (12), 132 (11), 131 (14), 130 (6), 120 (8), 118 (8), 117 (5), 107 (9), 106 (7), 91 (10), 65 (5).

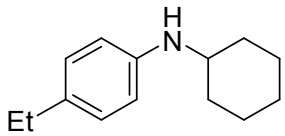

3dc (CAS registry number: 801192-87-0)

***N*-Cyclohexyl-4-ethylbenzenamine (3dc).** MS (70 eV, EI): *m/z* (%): 203 (50) [M^+], 204 (8), 188 (7), 161 (15), 160 (100), 147 (15), 134 (8), 132 (23), 131 (12), 130 (13), 118 (5), 106 (21), 105 (7), 91 (5), 79 (5), 77 (7).

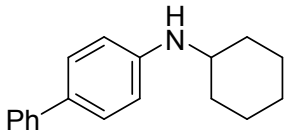

3ec (CAS registry number: 887748-95-0)

***N*-Cyclohexyl-[1,1'-biphenyl]-4-amine (3ec).** MS (70 eV, EI): *m/z* (%): 251 (82) [M^+], 252 (16), 209 (19), 208 (100), 195 (15), 194 (11), 193 (15), 182 (8), 180 (5),169 (17), 168 (8), 167 (9), 153 (6), 152

(12), 141 (6), 115 (6), 104 (6), 55 (5).

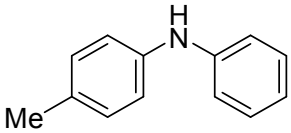

3be (CAS registry number: 620-84-8)

4-Methyl-*N*-phenylbenzenamine (3be). MS (70 eV, EI): *m/z* (%): 183 (100) [M^+], 184 (14), 182 (53), 180 (7), 168 (7), 167 (20), 91 (20), 90 (8), 77 (13), 65 (6), 51 (7).

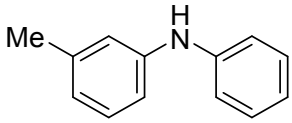

3ce (CAS registry number: 1205-64-7)

3-Methyl-*N*-phenylbenzenamine (3ce). MS (70 eV, EI): *m/z* (%): 183 (100) [M^+], 184 (14), 182 (28), 180 (6), 168 (16), 167 (35), 91 (11), 77 (9), 65 (6), 51 (5).

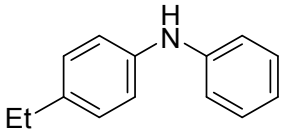

3de (CAS registry number: 32804-22-1)

4-Eethyl-*N*-phenylbenzenamine (3de). MS (70 eV, EI): *m/z* (%): 197 (50) [M^+], 198 (8), 183 (15), 182 (100), 180 (6), 168 (5), 167 (11), 91 (5), 90 (8), 77 (11), 51 (5).

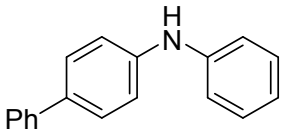

3ee (CAS registry number: 32228-99-2)

***N*-Phenyl-[1,1'-biphenyl]-4-amine (3ee).** MS (70 eV, EI): *m/z* (%): 245 (100) [M^+], 246 (20), 244 (20), 243 (6), 167 (6), 152 (5), 115 (5).

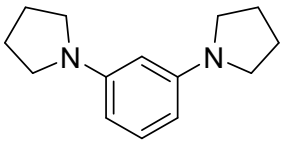

3fb (CAS registry number: 27594-18-9)

1,1'-(1,3-phenylene)bispyrrolidine (3fb). MS (70 eV, EI): *m/z* (%): 216 (100) [M^+], 217 (15), 215 (71), 189 (6), 188 (33), 187 (30), 174 (6), 173 (20), 161 (8), 160 (7), 147 (6), 146 (18), 145 (5), 132 (5), 118 (9), 117 (8), 108 (9), 107 (10), 104 (7), 91 (10), 86 (5), 77 (7), 65 (6).

Table S1 Hydrogenation of various hydrogen acceptors using Au–Pd/Al_2O_3[a]

Entry	Hydrogen acceptor	Hydrogenated product	Yield (%)
1	styrene	ethylbenzene	>99
2	**4aa**	**5aa**	65
3	1-octene	*n*-octane	63
4	cyclooctene	cyclooctane	66

[a] Reaction conditions: Au–Pd/Al_2O_3 (Au: 0.4 mol%, Pd: 0.6 mol% with respect to hydrogen acceptor), hydrogen acceptor (1.0 mmol), ethanol (2 mL), room temperature, H_2 (1 atm), 1 h. Yields were determined by GC analysis using *n*-decane as an internal standard.

Table S2 Results of the repeated reuse experiments for the dehydrogenative aromatization of **1a** with **2a**[a]

Au–Pd/Al_2O_3	Yield of **3aa** (%)	Average particle size (nm)
Fresh	76	2.9
First reuse	67	3.8
Second reuse	49	4.3

[a] The reaction was carried out under the conditions described in Fig. 3.

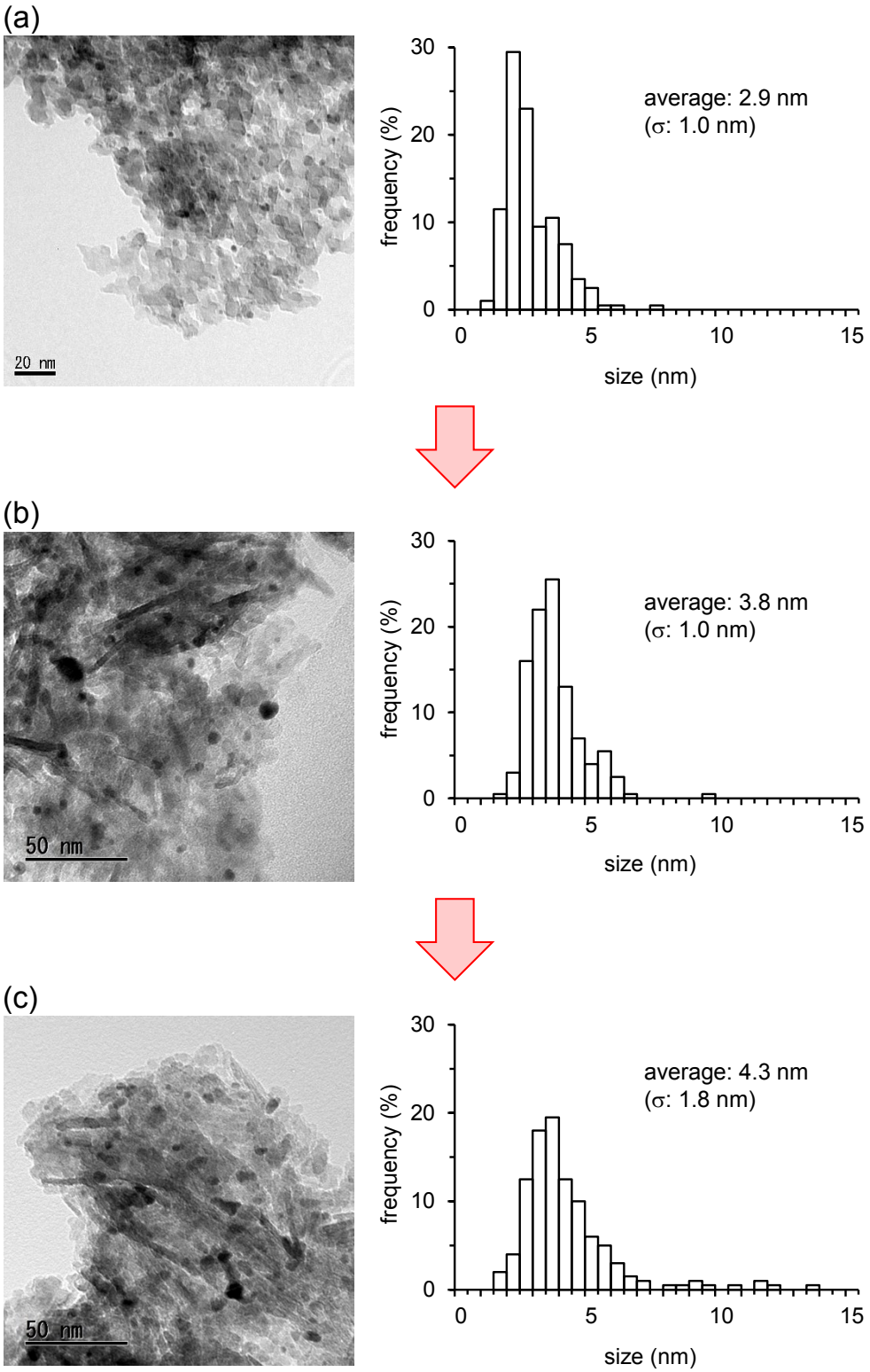

Fig. S1 TEM images of Au–Pd/Al_2O_3 and the size distributions of bimetallic nanoparticles. (a) Fresh (before the first use) (average: 2.9 nm, σ: 1.0 nm). (b) After the first use (average: 3.8 nm, σ: 1.0 nm). (c) After the second use (average: 4.3 nm, σ: 1.8 nm). The size distributions were determined using 200 particles.

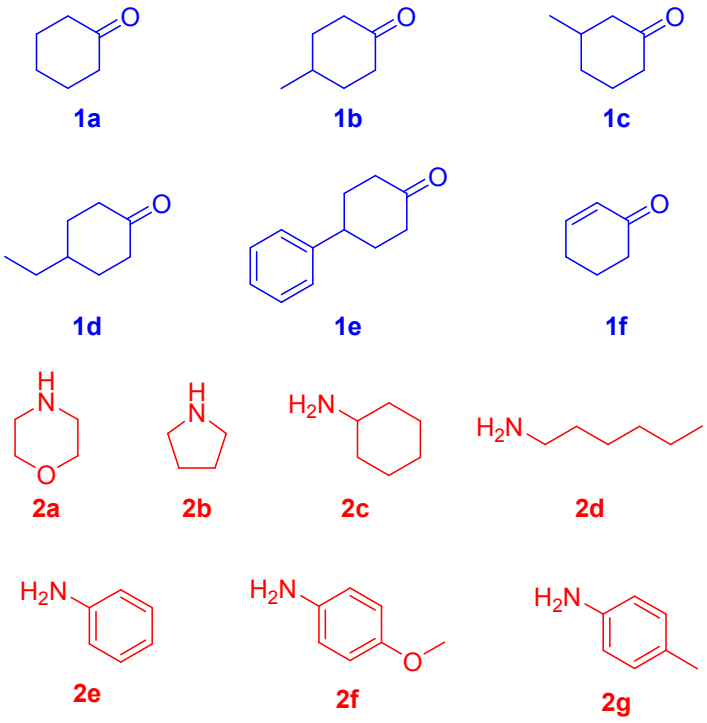

Fig. S2 Cyclohexanones and amines used in this study.

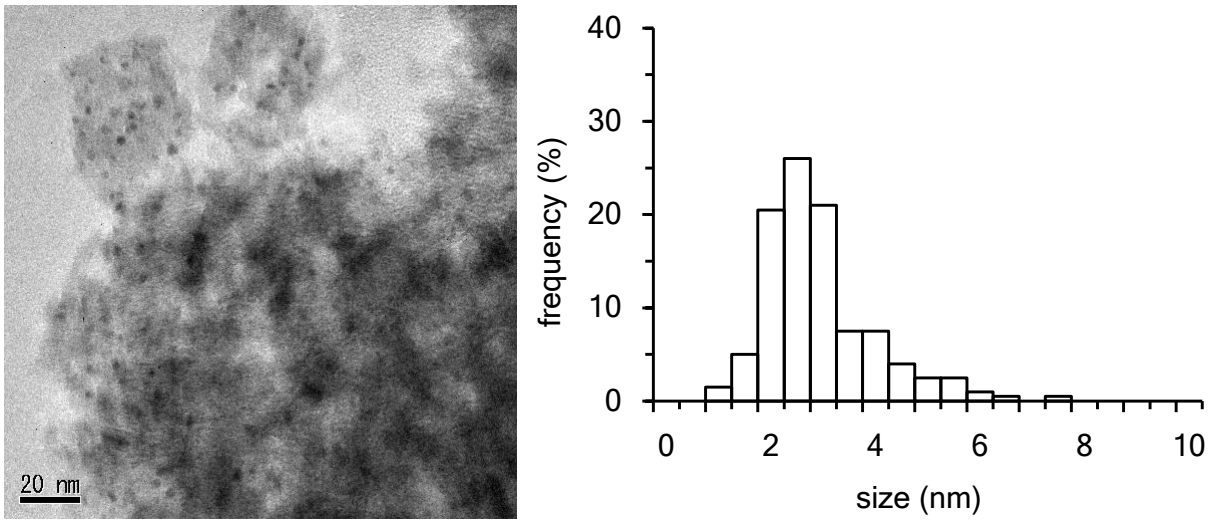

Fig. S3 TEM image of Au/Al_2O_3 and the size distribution of Au nanoparticles (average: 3.2 nm, σ: 1.1 nm). The size distribution was determined using 200 particles.

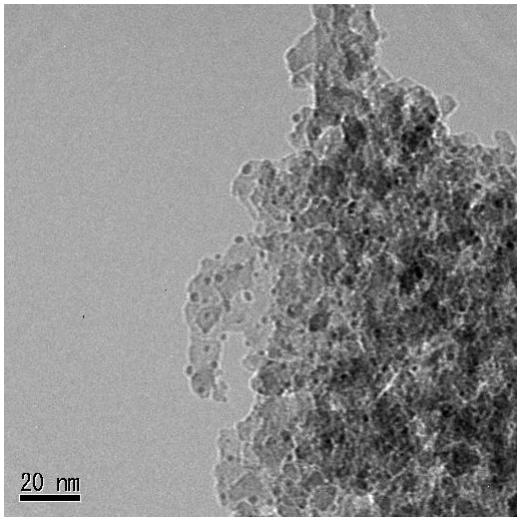

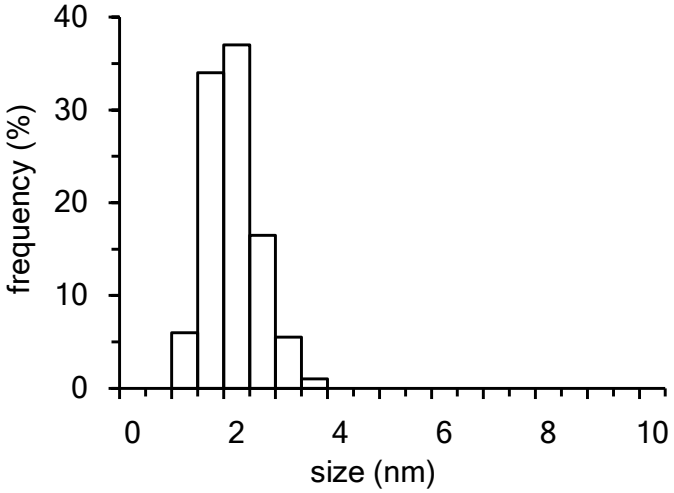

Fig. S4 TEM image of Pd/Al_2O_3 and the size distribution of Pd nanoparticles (average: 2.2 nm, σ: 0.5 nm). The size distribution was determined using 200 particles.

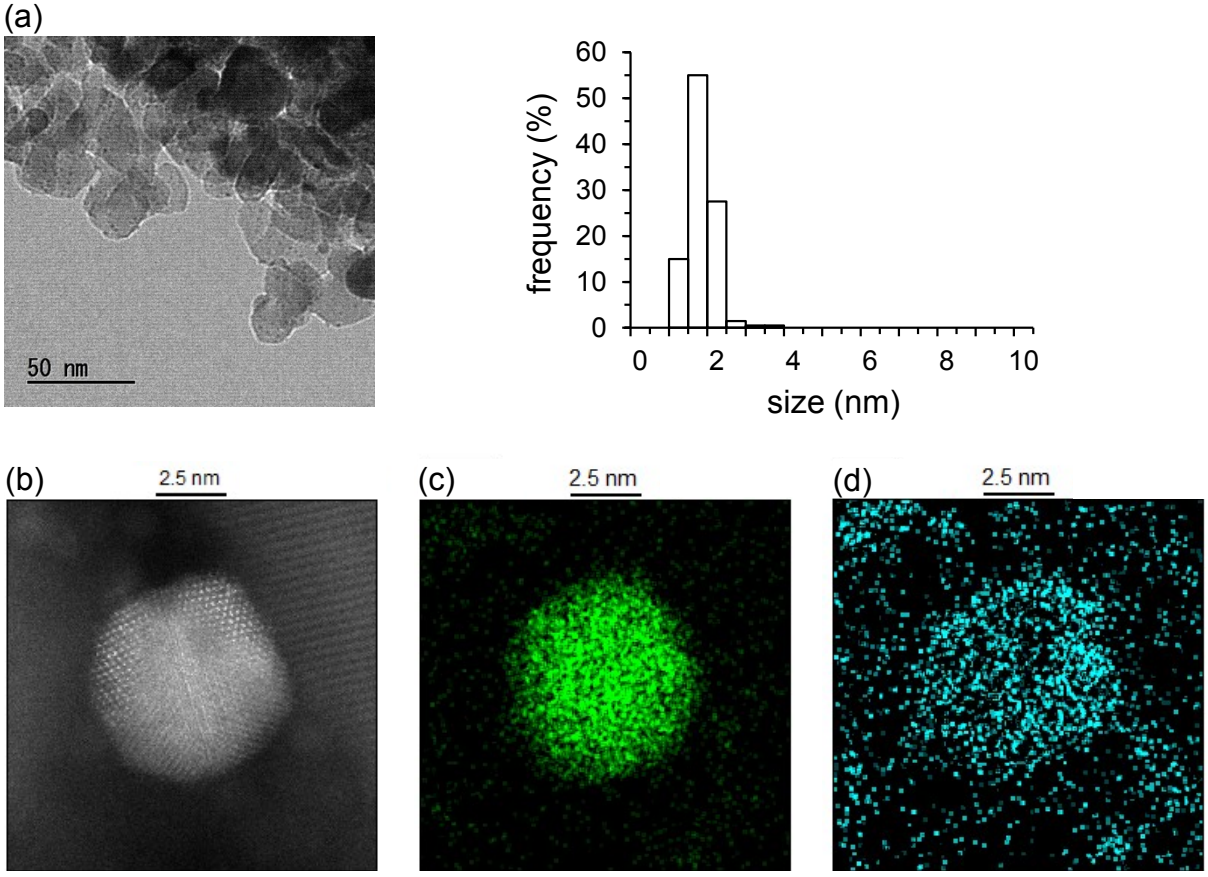

Fig. S5 (a) TEM image of Au–Pd/TiO_2 and the size distribution of bimetallic nanoparticles (average: 1.8 nm, σ: 0.4 nm). The size distribution was determined using 200 particles. (b) HAADF-STEM image of Au–Pd/TiO_2. (c) EDS images (Au element) of Au–Pd/TiO_2. (d) EDS images (Pd element) of Au–Pd/TiO_2. Green: Au, Blue: Pd.

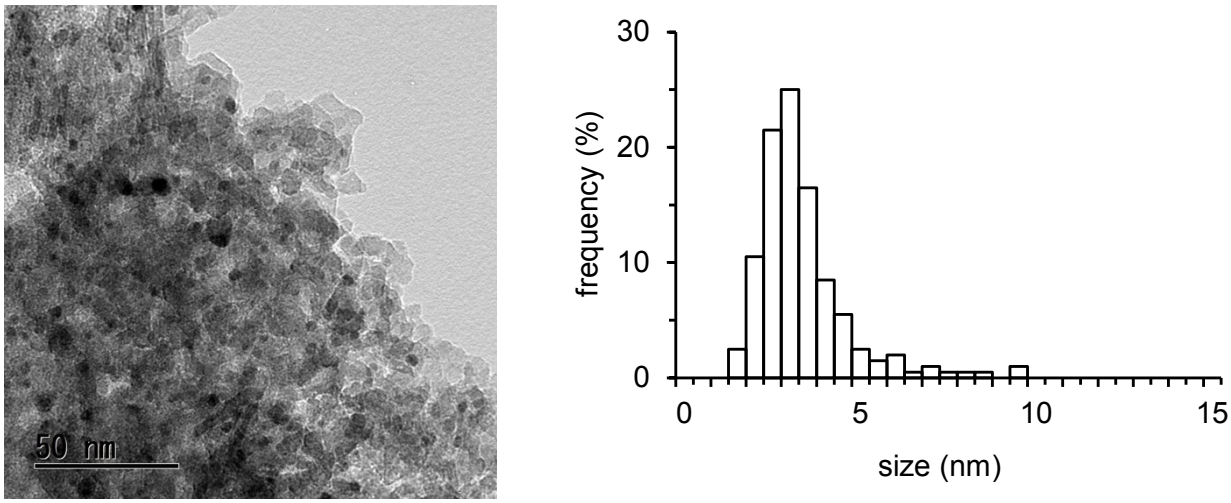

Fig. S6 TEM image of Au–Pd/$Al_2O_{3(Pd\rightarrow Au)}$ and the size distribution of bimetallic nanoparticles (average: 3.5 nm, σ: 1.3 nm). The size distribution was determined using 200 particles.

(a)

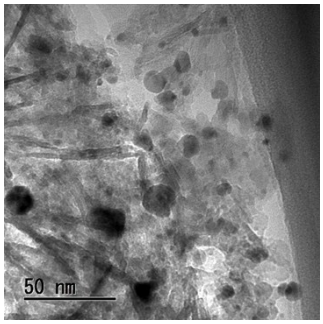
50 nm

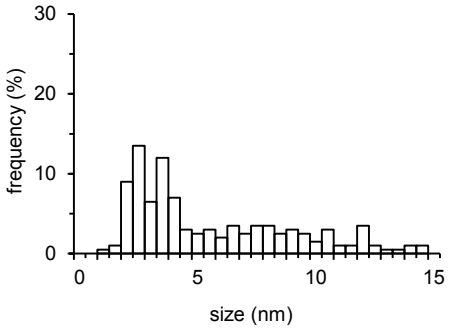
frequency (%)
30
20
10
0
0
5
10
15
size (nm)

(b)

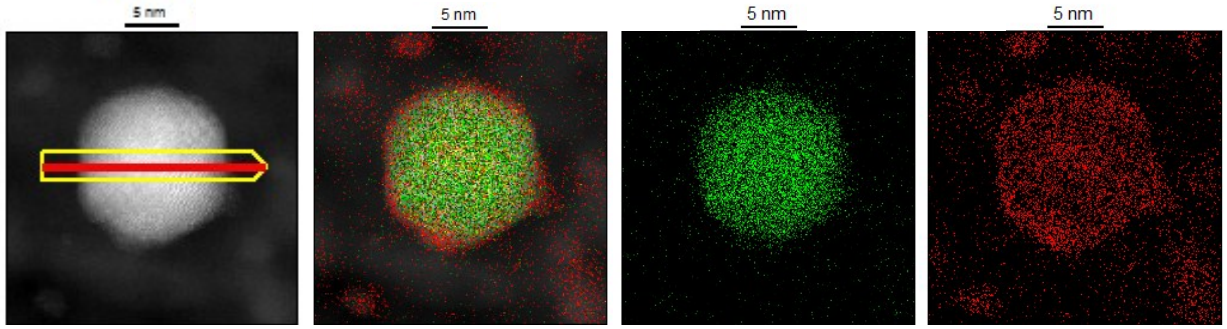
5 nm
5 nm
5 nm
5 nm

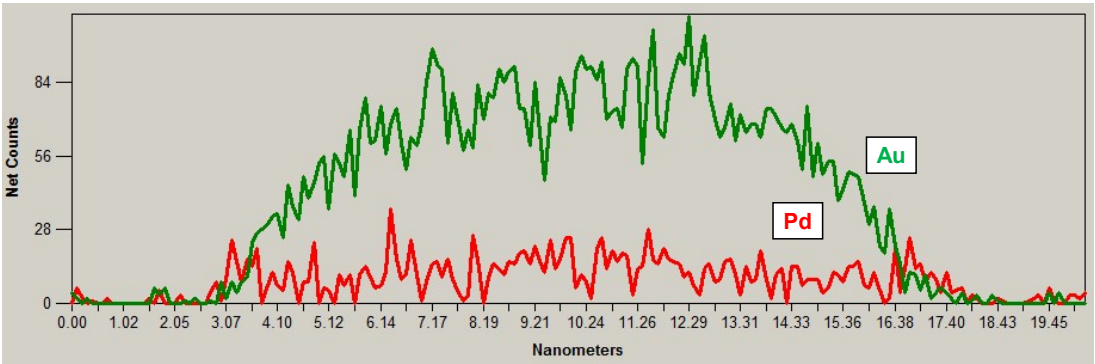
Net Counts
84
56
28
0
Au
Pd
0.00 1.02 2.05 3.07 4.10 5.12 6.14 7.17 8.19 9.21 10.24 11.26 12.29 13.31 14.33 15.36 16.38 17.40 18.43 19.45
Nanometers

(c)

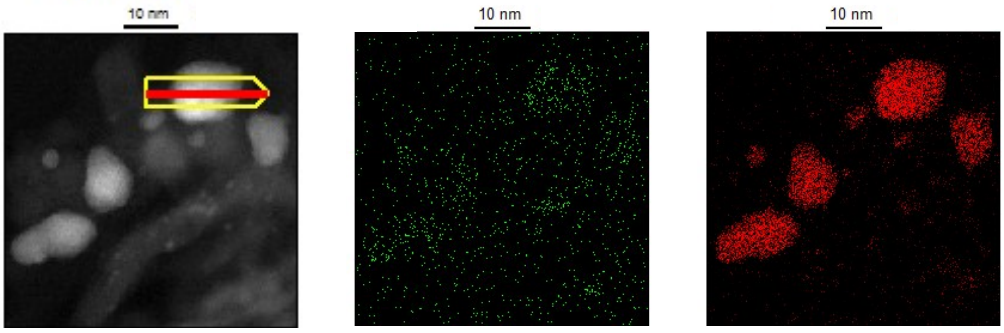
10 nm
10 nm
10 nm

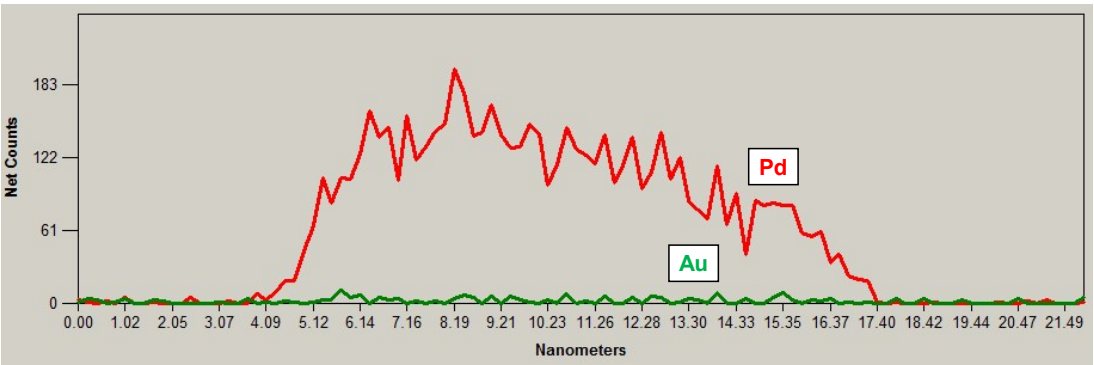
Net Counts
183
122
61
0
Pd
Au
0.00 1.02 2.05 3.07 4.09 5.12 6.14 7.16 8.19 9.21 10.23 11.26 12.28 13.30 14.33 15.35 16.37 17.40 18.42 19.44 20.47 21.49
Nanometers

(d)

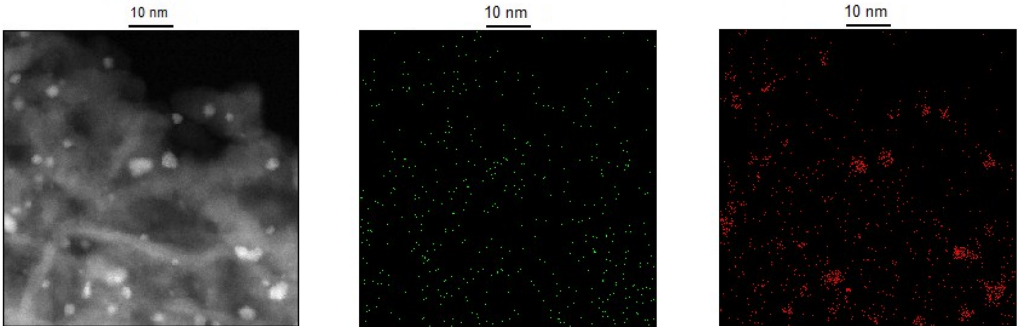

Fig. S7 (a) TEM image of Au–Pd/$Al_2O_{3(Au\rightarrow Pd)}$ and the size distribution of bimetallic nanoparticles. Au–Pd/$Al_2O_{3(Au\rightarrow Pd)}$ has wide size distribution (average: 6.3 nm, σ: 4.1 nm). The size distribution was determined using 200 particles. (b) HAADF-STEM and EDS images and cross-sectional compositional line profiles of large nanoparticles consisting of Au_{core}–Pd_{shell}. (c) HAADF-STEM and EDS images and cross-sectional compositional line profiles of large nanoparticles consisting of palladium. (d) HAADF-STEM and EDS images of small nanoparticles consisting of palladium. Green: Au, Red: Pd.

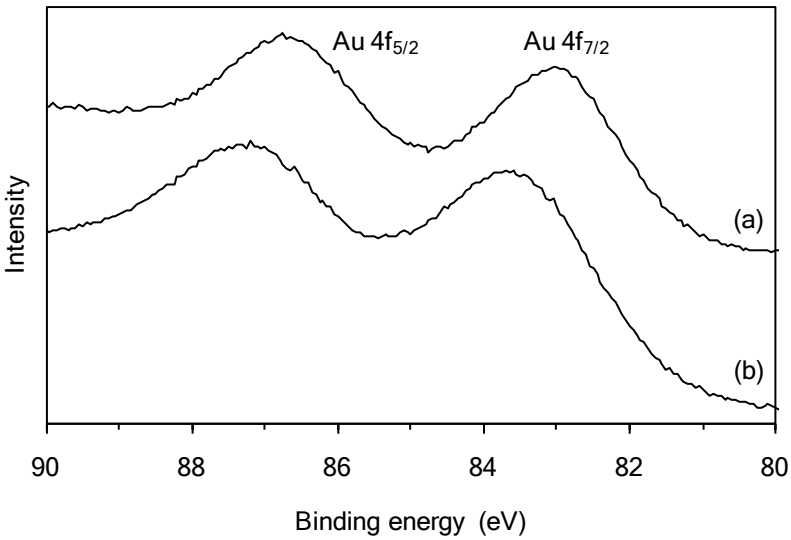

Fig. S8 XPS spectra of (a) Au–Pd/Al_2O_3 and (b) Au/Al_2O_3 around Au 4f components. The two peaks were attributed to Au $4f_{7/2}$ (around 83.0 eV) and $4f_{5/2}$ (around 87.0 eV). Au–Pd/Al_2O_3 exhibited negative shifts in the Au 4f binding energies in comparison with Au/Al_2O_3, suggesting the electron-transfer from palladium to gold atoms by alloying. Such phenomena have frequently observed for Au–Pd alloy nanoparticle catalysts (for example, see ref. 10).

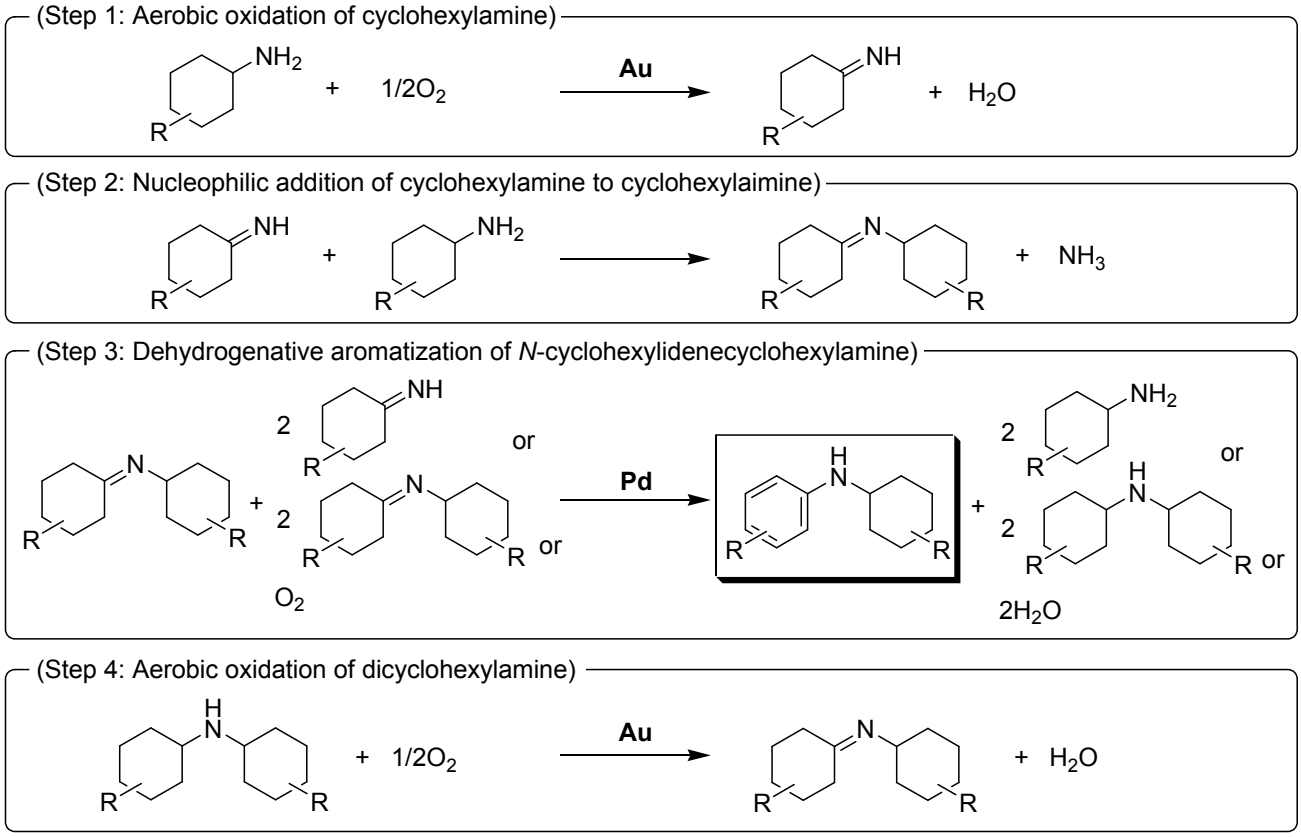

Scheme S1. Proposed reaction pathway for our recently reported Au–Pd/Al_2O_3-catalyzed dehydrogenative aromatization system from cyclohexylamines (see ref. 9). Initially, aerobic dehydrogenation of cyclohexylamine proceeds to give cyclohexylimine (step 1). Then, nucleophilic addition of another cyclohexylamine molecule to the cyclohexylimine intermediate takes place to afford *N*-cyclohexylidenecyclohexylamine (step 2). Finally, disproportionation and/or aerobic dehydrogenation of the *N*-cyclohexylidenecyclohexylamine proceeds to give the corresponding *N*-cyclohexylaniline as the final product with the concurrent formation of cyclohexylamine and dicyclohexylamine (step 3). These amines formed in the aromatization step can again aerobically be oxidized, and thus it can be considered that O_2 is formally the terminal oxidant (step 4).